SPATIAL RESOLUTION LIMITS OF YAG:CE POWDER BEAM-PROFILE MONITORS AT THE FERMILAB A0 PHOTOINJECTOR

A.H. Lumpkin, A.S. Johnson, J. Ruan, J. Santucci,Y.-E. Sun, and R. Thurman-Keup
Fermilab, Batavia, IL U.S.A. 60510

Abstract

The A0 photoinjector (A0PI) facility at Fermilab has an ongoing proof-of-principle experiment to demonstrate the exchange of the transverse horizontal and longitudinal emittances. This experiment relies on measurements of the transverse emittances and longitudinal emittance upstream and downstream of the exchanger beamline. At several locations along the accelerator beamline, YAG:Ce powder scintillator screens are used to determine beam size, divergence when the screen is downstream of a set of 50-micron-wide tungsten slits, and energy spread when used in an electron beam spectrometer. We have recently performed direct comparisons of beam image and slit image sizes using both the optical transition radiation (OTR) screens and the YAG:Ce screens. For micropulse charges of 250 pC and with beam energies of 15 MeV, we systematically observed larger beam image sizes with the YAG:Ce screens than with the OTR screens. We deduced a YAG:Ce screen spatial resolution limit of sigma = 140 to 180 microns. This term is large enough relative to the actual beam sizes and slit image sizes to be needed as a correction term subtracted in quadrature.

INTRODUCTION

The opportunity for a new series of beam characterization experiments at the Fermilab A0 photoinjector (A0PI) was recognized in the last year. There is an ongoing proof-of-principle experiment to demonstrate the exchange of the transverse horizontal and longitudinal emittances [1]. This experiment relies on measurements of the transverse emittances and longitudinal emittance upstream and downstream of an emittance-exchanger beamline. Generally, at the low beam energies of 14-15 MeV and emittances of 3-5 mm mrad one encounters beam sizes of 0.8 to 1.0 mm (sigma) [2,3]. Such beam sizes do not present a challenge to standard imaging procedures using scintillator screens or optical transition radiation screens. However, the use of 50-μm wide slits to sample the beam phase space followed by imaging at a downstream screen with a known drift distance to determine beam divergence [4] significantly alters the required resolution of the converter screen and imaging system. In this case, we deal with slit-image sizes of about σ =100 μm or less, and depending on the drift distance one deals with images that can approach the camera resolution limit or the scintillator resolution limit.

*Work supported by U.S. Department of Energy, Office of Science, Office of High Energy Physics, under Contract No. DE-AC02-06CH11357.

We have encountered both situations in recent transverse emittance experiments at A0PI using drifts between the slit location and the imaging screen of 0.39 and 0.80 m. Obviously, one prefers that the actual experimental beam sizes be at least three times larger than the uncorrelated limiting terms which can be treated in a quadrature sum [5]. When the limiting terms approach the observed value, one must subtract these contributions. In the past, the limiting term for Chromox powder screens was measured at the 200-μm level by comparing their beam images to those from OTR screens [6]. In addition, that work identified a saturation effect in YAG:Ce single crystals above a threshold areal charge density. We now present our evaluations of the YAG:Ce powder screen effects on the beam-size measurements in regard to beam divergence and beam energy spread. We have observed a systematically larger result with these screens than with OTR screens. There is extensive work on YAG:Ce screens for medical x-ray imaging that address spatial resolution versus screen thickness such as in reference [7] and references therein, but the x-rays have a more limited penetration depth than relativistic electrons.

EXPERIMENTAL BACKGROUND

The tests were performed at the Fermilab A0 photoinjector facility which includes an L-band photocathode (PC) rf gun and a 9-cell SC rf accelerating structure which combine to generate up to 16-MeV electron beams [1,3]. The drive laser operates at 81.25 MHz although the micropulse structure is usually counted down to 1 MHz. Due to the low, electron-beam energies and OTR signals, we typically summed over 50 micropulses with 0.25 nC per micropulse. The setup includes the upstream corrector magnets, quadrupoles, BPMs, the YAG:Ce/OTR imaging stations, and the beam dump as schematically shown in Fig. 1. The tests were performed in the straight-ahead line where beam-profiling stations designated as X3, X4, X5, and X6 are available after the accelerator. Initially, these were OTR stations except X5 had a YAG:Ce powder screen. The screens have ~5-micron grain size and are deposited with an ~ 50-micron thickness on a metal substrate as provided by DESY [8]. The powder screen is oriented with its surface normal at 45 degrees to the beam direction, and the camera views the front surface where the beam initially impinges. During the course of the experiments, we added an actuator with a dual screen capability at X5 to allow the direct comparisons of OTR and YAG:Ce, and we covered one half of the XS3 YAG:Ce screen with

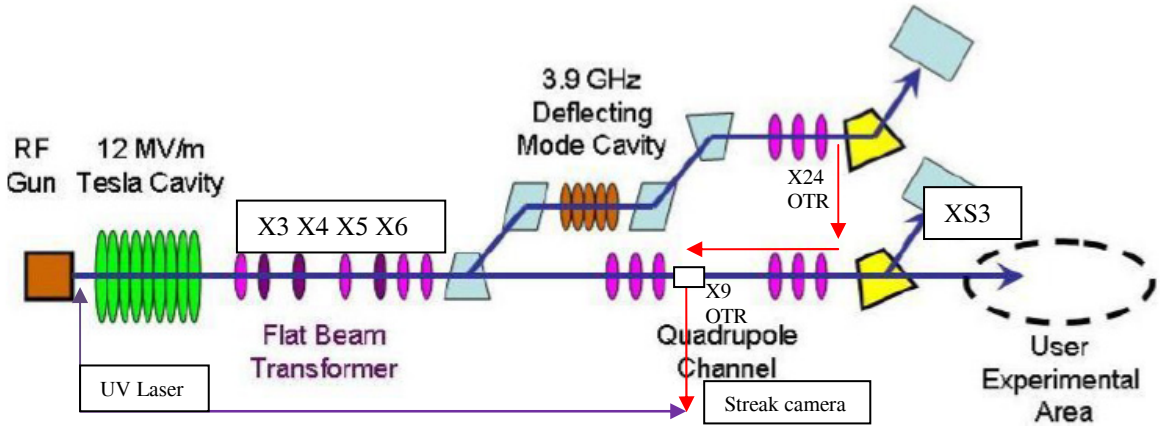

Figure 1: A schematic of the A0 photoinjector test area showing the PC rf gun, 9-cell Tesla cavity, transverse emittance stations, the OTR stations, the streak camera, and the second beamline when the two dogleg's dipoles are powered.

reflective Al foil to allow direct comparisons there as well. Energizing a downstream dipole sends the beam into a final beam dump and provides a spectrometer capability when combined with imaging of the beam size at the XS3 dispersive point in the focal plane. The dispersion in x is 324 mm, and the CCD calibration factor is 47.5 µm per pixel. This means a 0.1 % energy spread would correspond to an ~324-µm beam size after corrections are done. The initial sampling station was chosen at Cross#3, and an optical transport system using a 50-mm diameter field lens and a flat mirror brought the light to the firewire digital CCD camera.

Alternatively, the 4-dipoles of the emittance exchange (EEX) line could be powered and experiments done at an OTR Cross #23 after the fourth dipole and at a drift of 0.56m to Cross #24. The latter has both OTR and YAG:Ce powder screen options.

The OTR converter is an Al-coated optics mirror that is 1.5 mm thick with a zerodur substrate, and is mounted with its surface normal at 45 degrees to the beam direction on a stepper assembly. The assembly provides vertical positioning with an option for a YAG:Ce scintillator position. The charge was monitored by an upstream current monitor.

SYSTEM RESOLUTION EFFECTS

There are several contributions to the observed beam image size. When they are uncorrelated, the terms can be added in quadrature as described by Lyons [5]. The terms that have been considered are: actual (Act) image size, camera resolution (cam), YAG:Ce powder screen effects (YAG), and the finite slit width (slit) as shown in Eqs. 1, 2. In the spectrometer we must consider the finite size without dispersion, $\beta_x\varepsilon_x/\gamma$ where γ is the Lorentz factor, the dispersive term-energy spread product ($\eta_x\sigma_E$), and the system terms in Eqs. 3,4.

$$Obs^2 = Act^2 + YAG^2 + cam^2 + slit^2 \quad \text{Eq. 1}$$

Solving for the actual beam size we have,

$$Act = [Obs^2 - YAG^2 - cam^2 - slit^2]^{1/2} \quad \text{Eq. 2}$$

and in the spectrometer,

$$Obs^2 = Act^2 + YAG^2 + cam^2 + \beta_x\varepsilon_x/\gamma \quad \text{Eq. 3}$$

Solving for the actual beam size we have,

$$Act = [Obs^2 - YAG^2 - cam^2 - \beta_x\varepsilon_x/\gamma]^{1/2} = \eta_x\sigma_E \quad \text{Eq. 4}$$

In addition, there can be macropulse effects and OTR polarization effects which are addressed separately. Due to the large difference in conversion efficiency, we typically need to average over 50-100 micropulses for OTR images while only using 1-5 micropulses for the YAG:Ce screen. The potential for a smearing effect is high if the rf amplitude waveform is not flat to 0.1 % for the gun cavity and the 9-cell accelerator. We mention another potential effect at the 100-150 µm level of beam sizes. In analogy to some ODR and to high gamma OTR observations, we find the image size is reduced if one uses the orthogonal polarization component of the OTR. This is alluded to in reference [9] at the few-micron level, but empirically we have observed an effect at the 150-µm regime.

EXPERIMENTAL RESULTS

Chronologically, the first measurements that we did were in the spectrometer, XS3 after installation of the Al foil over half of the YAG:Ce screen located in the focal plane. We adjusted the 9-cell phase and the upstream quadrupoles for minimum observed beam size in the dispersive plane. We observed that the OTR image size was noticeably smaller at σ = 150 µm than the YAG image size at σ = 235 µm as shown in Fig. 2. This beam size includes the minimum spot size focus one could obtain. Although we did steer orthogonally to position the beam, we do not believe this would alter the focus this much. For the YAG:Ce we used one micropulse at 250 pC per micropulse, and for the OTR we obtained similar results for both 10- and 20-micropulse sums. With our micropulse spacing of about 1 µs this would be 10- and 20-µs-long macropulses, respectively.

At a later time we evaluated the change in this spot size in the dispersive direction with micropulse number. If the spot size grows this would indicate an energy slew during the macropulse. In Fig. 3 we show the observed image size for micropulse numbers from 10 to 150 for both 4-mm diameter drive laser spots (black curve) and 3-mm

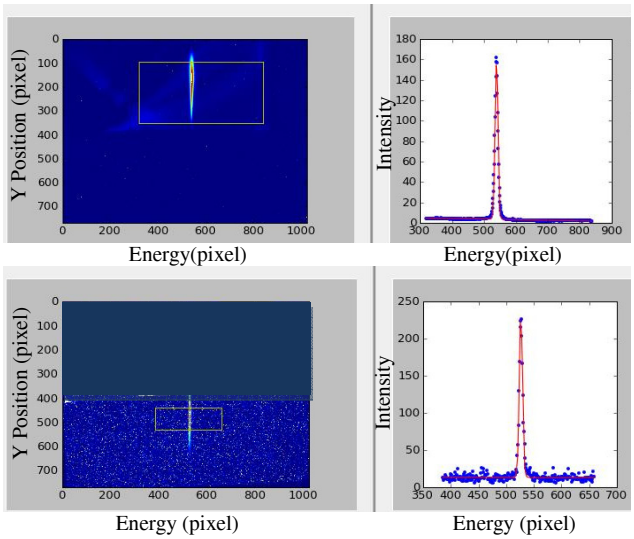

Figure 2: Initial comparison of XS3 images steered onto the YAG:Ce (top) and OTR foil (bottom). The observed narrow dimension beam sizes are 235 µm and 150 µm, respectively. The red curve is the Gaussian fit to the data profile.

diameter laser spots (red curve). A significant energy slew is indicated by the enlarging of the spot size with micropulse number. The timing for the rf modulator pulse was adjusted to present a flatter waveform, and the slew effect was dramatically reduced (green curve).

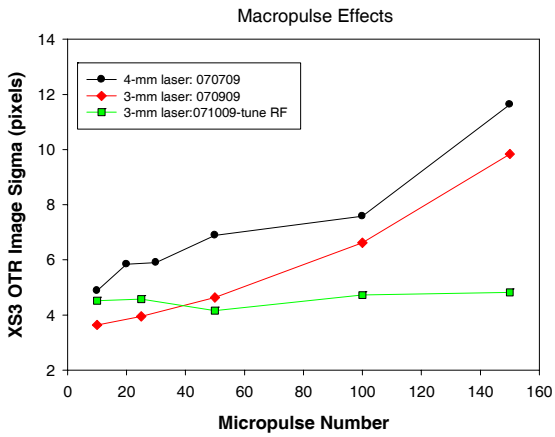

Figure 3: Variation of the observed beam image size in the dispersive plane of the spectrometer with the total number of micropulses in the macropulse.

The next tests used the dual screen capability in the X24 station in the EEX beamline. In this case we focused the beam to a stripe and evaluated the narrower dimension. The YAG:Ce screen again gave a larger image size (224 µm) than the OTR (138 µm) as shown in Fig. 4. The results are summarized in Table I. The estimated YAG:Ce resolution terms are 180 µm in XS3 and 176 µm in X24 for full images and charges. For actual beam sizes of 150 µm or less, a significant blurring has occurred in the YAG:Ce images.

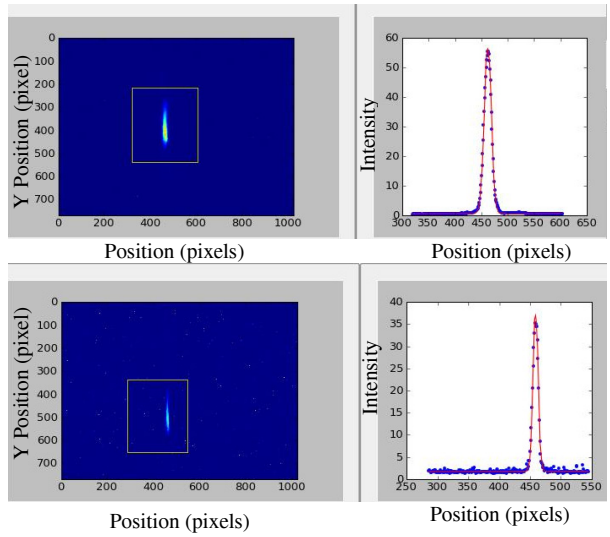

Figure 4: Comparison of the YAG:Ce (top) and OTR (bottom) images at X24 for 250 pC per micropulse. The observed narrow dimension beam sizes are 224 µm and 138 µm, respectively. The red curve is the Gaussian fit to the data profile.

Table I: Comparison of YAG:Ce and OTR beam images at 250 pC per bunch.

LOCATION	SCREEN	BUNCHES	SIGMA (pix)	SIZE(µm)
XS3	YAG	1	5.0	235
XS3	OTR	10	3.15	150
XS3	OTR	20	3.24	152
X24	YAG-2	1	7.0	224
X24	OTR	20	4.3	138

EMITTANCE RESULTS

We next evaluated the challenge with the combined beam size and slit image measurements at X3-X6. As stated before, the observed beam sizes at X3 after the accelerator were measured in the 800-µm regime in x and y. At this same station we have the capability to insert two slit assemblies, one with the 50-micron width for x divergence and one for y divergence. With the long length vertical we evaluate x divergence, and vice versa. In the initial measurements we have OTR screens at X3, X4, and X6 and a YAG:Ce powder at X5. As shown in Fig. 5 by the uncorrected data (L), the products of the beam size and divergence pairs are largest for the X5 cases. In addition, the X4 slit image sizes were in the 2-3 pixel range, close to the estimated camera resolution terms of 1.8-2.0 pixels. These terms were subsequently remeasured for the involved cameras and recalibrated. The YAG screen term was evaluated by correcting the X4 slit image for camera resolution and then multiplying this image size by the ratio of the drift distances for X5 and X4. This scaled image size was then subtracted in quadrature from the observed YAG slit image size to estimate its resolution term of about 160-180 µm. An example of the correction is shown in the equation following for the X3-X5 pair:

$$\varepsilon^{n}{}_{x} = \gamma\sigma_{x}(\mathrm{x3})\sigma_{x}(\mathrm{x5 - Vslits})/0.80\ \mathrm{m}$$
$$= 28 \cdot 0.73\,\mathrm{mm} \cdot \frac{6.82\ \mathrm{pixels} \cdot 0.0268\ \mathrm{mm/pixel}}{0.80\ \mathrm{m}}$$
$$= 4.7\,\mathrm{mm\ mrad} \Rightarrow 2.0\ \mathrm{mm\ mrad}$$

when X5 corrected to 2.84 pixels using 160 μm for the YAG : Ce resolution term and 1.8 pixels for the camera resolution term.

For the OTR data we had to use 100 micropulses for X4 and 150 micropulses for X6 so macropulse effects can be involved. The corrected results are shown in the plots at the right in Figs. 5 and 6 for the x and y emittances, respectively. In both planes, the corrected emittances are ~3 mm mrad for the central solenoid currents. The data have the smallest. The X6 data involve the longest drift so the image size is sufficiently larger than the camera resolution term so it's only a small correction.

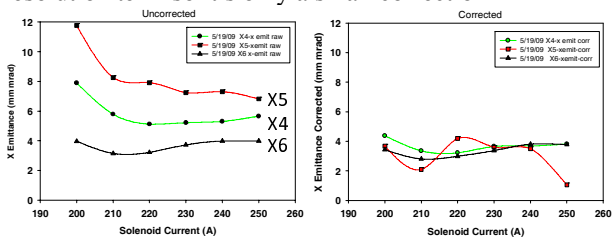

Figure 5: Plots of the variation of the uncorrected (L) and corrected (R) x emittances calculated from the product of the X3 beam size and the divergences determined at X4 (green), X5 (red), and X6 (black) with solenoid current.

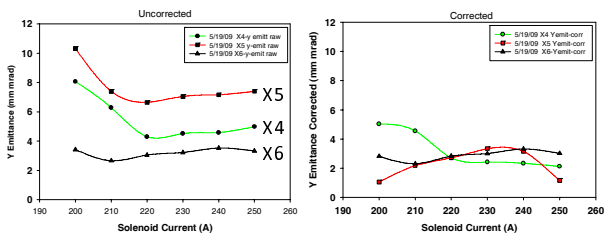

Figure 6: Plots of the variation of the uncorrected (L) and corrected (R) y-emittances calculated from the product of the X3 y beam size and the divergences determined at X4 (green), X5 (red), and X6 (black) with solenoid current.

OTR POLARIZATION EFFECTS

We have also initial data on the effects of using the orthogonal OTR polarization component for the beam size dimensions. We systematically observe smaller beam images by 10-20 µm with the orthogonally polarized light than with the total OTR for slit images. Since the slit images are in the range of 100 µm, this is an additional size correction. We believe these are the first reports of the effect at such low gamma, although Castellano and Verzilov evaluated a polarization effect at the single-particle-function level and at the few-micron level for a range of beam energies [9].

SUMMARY

In summary, we have investigated the contributions of several terms to beam profile station system resolution at A0PI. In order to reconcile the data taken with different screens in the spectrometer and in the EEX line, we hypothesized a limiting YAG:Ce powder screen resolution term of σ=140-180 µm as deduced from quadrature analyses and applying a camera resolution term of 1.8-2.2 pixels. These are relevant for narrow beam images at XS3 and X24. The slit images are more of a challenge, but the initial comparisons also imply YAG:Ce powder screen terms of 100-160 microns. The measurements are complicated by the need to use 50 -100 bunches for the OTR screen while only using 1-5 bunches for the YAG:Ce screen and potential OTR polarization effects. Macropulse effects are clearly in play in the spectrometer, and we expect them in the slit images since upstream correctors are involved. We recommend application of such corrections to earlier 250-pC data as warranted. Further investigations are anticipated after the rf amplitude and phase envelopes for the gun and accelerator are reliably flattened.

ACKNOWLEDGEMENTS

The authors acknowledge support from M. Wendt, H. Edwards, and M. Church of Fermilab as well as A0 technical software assistance from M. Davidsaver.

REFERENCES

[1] T. Koeth, L. Bellantoni, D. Edwards, H. Edwards, R. P. Fliller III, " A TM110 Cavity for Longitudinal to Transverse Emittance Exchange", PAC 07, THPAS079, Albuquerque , NM , USA.

[2] Tikohoplav Rodion, PhD thesis, "Low Emittance Electron Beam Studies", FERMILAB-THESIS-2006-04.

[3] R. P. Fliller, H. Edwards, W. Hartung, "Time dependent quantum efficiency and dark current measurements in an RF Photocathode injector with a high quantum efficiency cathode", JACoW, Proc. of PAC05, Knoxville, USA.

[4] C.H. Wang et al., "Slits Measurement of Emittance on TTF", International Conference on Accelerator and Large Experimental Physics Control Systems, Trieste, Italy (1999).

[5] L. Lyons, Statistics for Nuclear and Particle Physicists (1986).

[6] A.H. Lumpkin, W.J. Berg, B.X. Yang, and M.White, Proc. of Linac98, 529, JACoW (1998).

[7] I. Kandarakis et al., Nucl. Instr. Meth. in Phys. Res. **A538**, 615 (2005).

[8] K.Floettmann of DESY provided the powder screens which are described in R. Spesyvtsev's Master's Thesis,"Transverse Beam Size Measurement Systems at Photo Injector Test Facility in Zeuthen" (2007).

[9] M. Castellano and V.A.Verzilov, Phys. Rev. ST Accel. Beams, 1:062801 (1998).